Adaptive Solid-State Structures

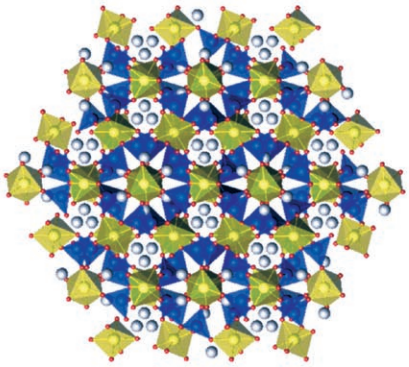

Garnet

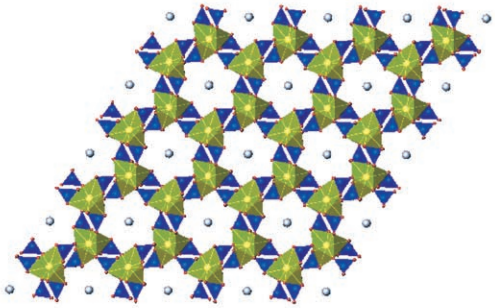

Apatite

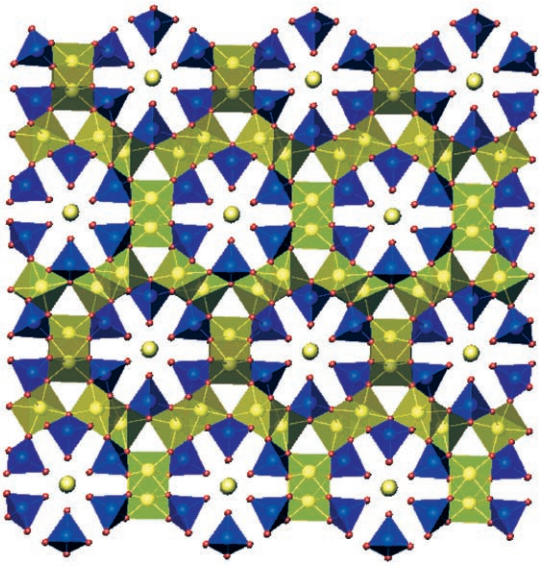

Lyonsite

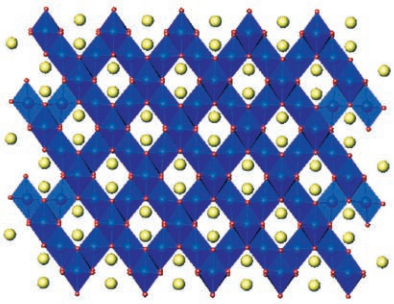

Spinel

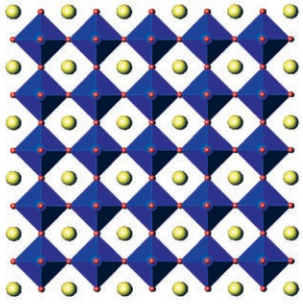

Perovskite

DOI: 10.1002/chem.200600294

The Adaptable Lyonsite Structure

Jared P. Smit, Peter C. Stair, and Kenneth R. Poeppelmeier*[a]

Abstract: Crystal frameworks that can accommodate a wide range of elements, oxidation states, and stoichiometries are an important component of solid-state chemistry. These frameworks allow for unique comparisons of different metal-cation compositions with identical atomic arrangements. The mineral Lyonsite, α-$Cu_3Fe_4(VO_4)_6$, is emerging as the archetypal framework structure for a large class of materials, similar to known frameworks such as perovskite, garnet, apatite, and spinel. The new lyonsite-type oxides $Li_{2.82}Hf_{0.795}Mo_3O_{12}$ and $Li_{3.35}Ta_{0.53}Mo_3O_{12}$, in which hafnium and tantalum retain their highest oxidation states, are presented to advance the concept of the lyonsite structure as an adaptable framework.

Keywords: cations · ceramics · solid-state reactions · solid-state structures · X-ray diffraction

Introduction

Minerals such as perovskite ($CaTiO_3$), garnets ($A_3B_2(SiO_4)_3$), apatites ($A_5(BO_4)_3X$), and spinel ($MgAl_2O_4$) are the archetypal structures for large numbers of materials with different chemical compositions within each structure type. Each has been reviewed extensively.[1–8] Oxide classes such as these can accommodate a wide variety of metal cations while retaining their unique structure, and are well-studied for various properties afforded by this versatility. Properties can often be tuned or changed by elemental substitution, and materials with the same structural connectivity can be studied for different purposes. A lesser known, but ubiquitous structure type with similar adaptive properties takes its name from the mineral Lyonsite, α-$Cu_3Fe_4(VO_4)_6$.[9] While the properties resulting from the lyonsite structure in molybdates have been discussed previously in a brief review on different families of $A_xB_y(MoO_4)_z$ molybdates,[10] this concept will focus on the adaptable nature of the lyonsite crystal framework, including the presentation of the new lyonsite type structures $Li_{2.82}Hf_{0.795}Mo_3O_{12}$ and $Li_{3.35}Ta_{0.53}Mo_3O_{12}$.

The general formula for lyonsite-type oxides can be written as $A_{16}B_{12}O_{48}$ ($A_{16}(BO_4)_{12}$), in which the oxygen framework creates three different A sites that are typically (but not limited to) lower oxidation-state (+1, +2, +3) metal cations enclosed in edge-sharing octahedra, edge-sharing trigonal prisms, and face-sharing octahedra. High-oxidation-state cations (+5, +6) occupy the two unique tetrahedrally coordinated B sites. The structural connectivity of lyonsite-type oxides is based on an array of pseudohexagonal oxygen atoms, and built up of isolated BO_4 tetrahedra linked by AO_6 chains, which can be seen in Figure 1. The most unique features of the structure are the hexagonal tunnels that con-

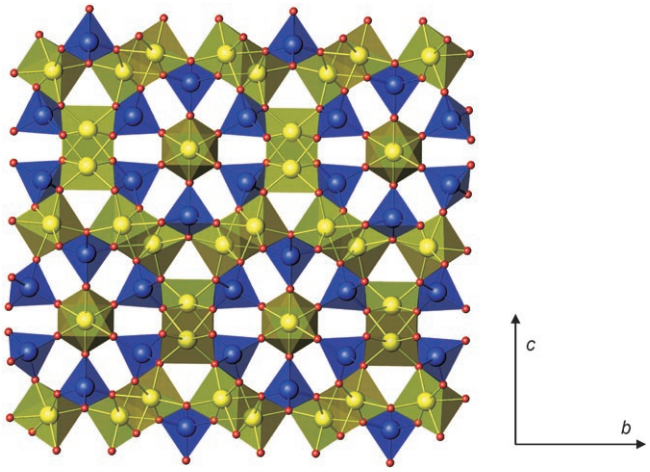

Figure 1. The lyonsite structural framework and connectivity. yellow polyhedra represent AO_6 polyhedra and blue polyhedra represent BO_4 tetrahedra.

[a] J. P. Smit, Prof. P. C. Stair, Prof. K. R. Poeppelmeier
Department of Chemistry, Northwestern University
2145 Sheridan Road, Evanston, Illinois 60208–3113 (USA)
Fax: (+1) 847-491-7713
E-mail: krp@northwestern.edu

Supporting information for this article is available on the WWW under http://www.chemeurj.org or from the author.

sist of AO_6 polyhedra. Two sides of the hexagonal tunnel are created by zigzag sheets of edge-sharing A-centered trigonal prisms, while the remaining four sides are composed of columns of edge-sharing A-centered octahedra. Isolated BO_4 tetrahedra are joined to the inside of the tunnel, and infinite chains of face shared AO_6 octahedra pass through the center of these tunnels.

The number of different cations known to occupy the six-coordinate A position is extensive, and these cations are listed in Table 1. The identity of the A-site cation seems to depend almost exclusively on size ($0.46 \leq r(A^{n+}) \leq 1.02$ Å).[11] If Na^+ and Cu^+ are excluded, the size range becomes rather narrow ($0.53 \leq r(A^{n+}) \leq 0.79$ Å).[11] As illustrated in Table 1, the cation charge has almost no effect on the identity of A, with cations of oxidation state +1 through +4 shown to occupy the six-coordinate positions. In this concept article, it is shown that Hf^{4+} and Ta^{5+} (a pentavalent cation) can occupy the A-centered AO_6 polyhedra. It appears that nearly any cation can be used for this position if it is of suitable size. However, charge balance must always be maintained, and A is rarely a single type of cation. Generally, A is a combination of two cations of different oxidation states arranged such that the total composition is charge neutral. The B site is limited to smaller, highly charged ions that are able to form BO_4 tetrahedra. To date, V^{5+}, Mo^{6+}, and W^{6+} have been found to occupy the B site, and it is likely that similarly sized, highly charged cations (As^{5+}, P^{5+}, Si^{4+}, etc.) will also be found to fill that position.

Table 1. A-site cations.

Oxidation state	Element	Size [Å][11]	Reference(s)
+1	Li	0.74	[13–29, 46–48, 51], this work
	Na	1.02	[12, 14]
	Cu	0.46	[30]
+2	Mg	0.72	[15, 16, 19, 31, 32, 46–48, 51]
	Mn	0.67	[17, 18, 34]
	Fe	0.77	[13, 15]
	Co	0.74	[12, 15, 17, 20, 36–38, 40]
	Ni	0.70	[15, 17, 21]
	Cu	0.73	[9, 14, 30, 39]
	Zn	0.75	[14, 15, 35]
+3	Al	0.53	[23, 24]
	Sc	0.73	[23, 26]
	Cr	0.62	[24, 39, 40]
	Fe	0.65	[9, 13, 23, 24, 37, 38, 39]
	Ga	0.62	[23, 24]
	Co	0.61	[12, 25, 29]
	In	0.79	[23]
+4	Ti	0.61	[27]
	Zr	0.72	[16, 27, 28]
	Hf	0.71	[16, 27], this work
+5	Nb	0.64	this work
	Ta	0.64	this work

Lyonsite-Type Oxides—A Historical Perspective

Molybdates: A timeline of the lyonsite structure is listed in Table 2. The largest percentage, by a wide margin, of the existing lyonsite-type compounds are molybdates. Not surprisingly then, the structure was first discovered, recognized as a new structure type, and described for $NaCo_{2.31}(MoO_4)_3$ by Ibers and Smith in 1964.[12] In 1970, the crystal structures of $Li_3Fe(MoO_4)_3$ and $Li_2Fe_2(MoO_4)_3$ were described, and the structural similarity to $NaCo_{2.31}(MoO_4)_3$ was noted.[13] Shortly following, $Li_2M^{2+}{}_2(MoO_4)_3$ (M = Mg, Mn, Co, Ni, Cu, Zn),[14–22] $Li_3M^{3+}(MoO_4)_3$ (M = Al, Cr, Ga, Sc, In, Co),[23–26] and $Li_2M^{4+}(MoO_4)_3$ (M = Ti, Zr, Hf)[27,28] were discovered by comparing their powder diffraction patterns to the powder diffraction patterns of $Li_2Fe_2(MoO_4)_3$ and $Li_3Fe(MoO_4)_3$. In many cases, the crystal structures have since been determined (see Table 2). However, most of the lyonsite type molybdates are

Table 2. Lyonsite timeline.

Reported crystal structure				Reported powder phase		
Year	Phase(s)	% A Site Vacant	Ref.	Year	Phase(s)	Ref.
1964	$NaCo_{2.31}(MoO_4)_3$	17.25	[12]	1970	$Li_3Fe(MoO_4)_3$	[23]
1970	$Li_3Fe(MoO_4)_3$	0	[13]	1970	$Li_3Al(MoO_4)_3$	[23]
1970	$Li_2Fe_2(MoO_4)_3$	0	[13]	1970	$Li_3Sc(MoO_4)_3$	[23]
1971	$Cu_{3.85}Mo_3O_{12}$	3.75	[30]	1970	$Li_3Ga(MoO_4)_3$	[23]
1977	$Li_2Ni_2(MoO_4)_3$	0	[21]	1970	$Li_3In(MoO_4)_3$	[23]
1978	$Li_2Zr(MoO_4)_3$	25	[28]	1971	$Li_3Fe(MoO_4)_3$	[24]
1987	$Cu_3Fe_4(VO_4)_6$	12.5	[9]	1971	$Li_3Al(MoO_4)_3$	[24]
1994	$Li_2Mg_2(WO_4)_3$	0	[46]	1971	$Li_3Ga(MoO_4)_3$	[24]
1994	$Mg_{2.5}VMoO_8$	6.25	[31]	1971	$Li_3Cr(MoO_4)_3$	[24]
1994	$Li_{1.6}Mn_{2.2}(MoO_4)_3$	5	[18]	1971	$Li_2Mg_2(MoO_4)_3$	[16]
1995	$Li_2Co_2(MoO_4)_3$	0	[20]	1971	$Li_2Mg_2(WO_4)_3$	[16]
1996	$Mg_{2.54}V_{1.08}Mo_{0.92}O_8$	4.75	[32]	1971	$Li_{10}Zr_2(MoO_4)_9$	[16]
1997	$Zn_{3.77}V_{1.54}Mo_{1.46}O_{12}$	5.75	[35]	1971	$Li_{10}Hf_2(MoO_4)_9$	[16]
1998	$Mn_{2.47}V_{0.94}Mo_{1.06}O_8$	7.375	[34]	1972	$Li_2Zn_2(MoO_4)_3$	[14]
2000	$Co_4Fe_{3.33}(VO_4)_6$	8.375	[37]	1972	$Li_2Cu_2(MoO_4)_3$	[14]
2001	$Cu_4Fe_{3.333}(VO_4)_6$	8.3375	[39]	1972	$Na_2Zn_2(MoO_4)_3$	[14]
2001	$Cu_{4.05}Cr_{3.3}(VO_4)_6$	8.125	[39]	1972	$Na_2Cu_2(MoO_4)_3$	[14]
2002	$Co_{3.6}Fe_{3.6}(VO_4)_6$	10	[38]	1973	$Li_2Zr(MoO_4)_3$	[27]
2003	$Co_5Cr_{2.667}(VO_4)_6$	4.1625	[40]	1973	$Li_2Hf(MoO_4)_3$	[27]
2003	$Li_2Mg_2(MoO_4)_3$	0	[19]	1973	$Li_2Ti(MoO_4)_3$	[27]
2003	$Li_3Sc(MoO_4)_3$	0	[26]	1976	$Li_2Mn_2(MoO_4)_3$	[17]
2003	$Co_{2.5}VMoO_8$	6.25	[36]	1976	$Li_2Co_2(MoO_4)_3$	[17]
2005	$Mg_{2.56}V_{1.12}W_{0.88}O_8$	4	[48]	1976	$Li_2Ni_2(MoO_4)_3$	[17]
2006	$Li_{2.82}Hf_{0.795}(MoO_4)_3$	9.625	this work	1977	$Li_2Zn_2(MoO_4)_3$	[15]
2006	$Li_{3.35}Ta_{0.53}(MoO_4)_3$	3	this work	1977	$Li_2Mg_2(MoO_4)_3$	[15]
				1977	$Li_2Co_2(MoO_4)_3$	[15]
				1977	$Li_2Ni_2(MoO_4)_3$	[15]
				1977	$Li_2Fe_2(MoO_4)_3$	[15]
				1992	$Li_3Co(MoO_4)_3$	[25]
				2006	$Li_{3.5-5x}Nb_{0.5+x}(MoO_4)_3$	this work

still only known from their powder X-ray diffraction patterns.

In addition to the large class of lithium compounds, the lyonsite-type sodium molybdates $Na_{2-2x}Co_{2+x}(MoO_4)_3$ and $Na_{2-2x}Zn_{2+x}(MoO_4)_3$,[14] are also known, and the original $NaCo_{2.31}(MoO_4)_3$ structure is likely a variation of these solid solutions. Klevtsova and Magarill have suggested that the true composition for $NaCo_{2.31}(MoO_4)_3$ is likely to be $Na_2Co_2(MoO_4)_3$ ($x=0$),[13] although the composition $NaCo_{2.5}(MoO_4)_3$ ($x=0.5$) would probably be more consistent with the original study. However, the presumption of Co^{3+} cannot be ruled out, as Co^{3+} can occupy the A site.[25,29]

The only known lyonsite-type molybdate with only one cation in the octahedral/trigonal prismatic positions was one of the first lyonsite compounds discovered: $Cu_{3.85}Mo_3O_{12}$, discovered in 1971.[30] This is unusual because the A site is usually occupied by a combination of two cations. However, $Cu_{3.85}Mo_3O_{12}$ requires the presumption of Cu^+, and the monovalent cation is consistent with other lyonsite type molybdates. While one of the A site cations in lyonsite type molybdates is always monovalent, the remaining cation is quite flexible. It appears that a monovalent cation is required for the lyonsite-type molybdates, because the $(MoO_4)^{2-}$ anion is not highly charged. The formula of $A_4(MoO_4)_3$ requires that A have an average charge of only +3/2. The A site can be under occupied (cation vacancies), as discussed later, which is one way of decreasing the average charge. However, cation vacancies can only be tolerated to a certain extent before any crystal framework will collapse, and the best way for lyonsite-type molybdates to have an average charge of +3/2 on the A site is to incorporate a monovalent cation.

Vanadates and vanadomolybdates: α-$Cu_3Fe_4(VO_4)_6$ was discovered in 1987, but no reference was made to the relationship between this new mineral and the large family of molybdates. This is not surprising owing to their dissimilar chemical compositions (α-$Cu_3Fe_4(VO_4)_6$ and $NaCo_{2.31}(MoO_4)_3$). It is, indeed, quite remarkable that such different compositions could retain the same structure. Nonetheless, the discovery of the mineral suggested that V^{5+} could be used in place of Mo^{6+} for the tetrahedral cation. It was not until 1994, when phase relation studies in the $Mg_3(VO_4)_2$–$MgMoO_4$ system revealed the mixed lyonsite type vanadomolybdate phase $Mg_{2.5}VMoO_8$, as well as the simultaneous structural refinement of $Li_{1.60}Mn_{2.20}(MoO_4)_3$, that the nonevident connection was made between α-$Cu_3Fe_4(VO_4)_6$ and $NaCo_{2.31}(MoO_4)_3$.[18,31,32]

After the early 1990s, when $Mg_{2.5}VMoO_8$ was shown to be effective for the oxidative dehydrogenation of alkane hydrocarbons,[33] searches for other potentially catalytically active phases focused on the lyonsite structure type and the phases $M_{2.5}VMoO_8$ (M = Mn, Zn, Co) were soon discovered.[34–36] In addition to mixed vanadomolybdates, lyonsite-type vanadates were also targeted, and the vanadates $Co_4Fe_{3.33}(VO_4)_6$,[37] $Co_{3.6}Fe_{3.6}(VO_4)_6$,[38] $Cu_4Fe_{3.333}(VO_4)_6$,[39] $Cu_{4.05}Cr_{3.3}(VO_4)_6$,[39] and $Co_5Cr_{2.667}(VO_4)_6$[40] were all recognized to be isostructural with $NaCo_{2.31}(MoO_4)_3$ and α-$Cu_3Fe_4(VO_4)_6$.

Interestingly, attempts to synthesize α-$Cu_3Fe_4(VO_4)_6$ resulted in a different phase, β-$Cu_3Fe_4(VO_4)_6$,[41] with the $Fe_7(PO_4)_6$[42] structure type. Most likely, the mineral could not be synthesized for one of two reasons, or a combination therein. First, comparing the density of α-$Cu_3Fe_4(VO_4)_6$ (4.21 $g\,cm^{-3}$) and β-$Cu_3Fe_4(VO_4)_6$ (3.97 $g\,cm^{-3}$), Lafontaine et al. suggested that α-$Cu_3Fe_4(VO_4)_6$ may be a high-pressure phase.[41] Many vanadates have since been discovered that are isostructural with β-$Cu_3Fe_4(VO_4)_6$ such as $M_3Fe_4(VO_4)_6$ (M = Mn, Mg, Zn, Co),[37,43,44] while no stoichiometric $A_3B_4(VO_4)_6$ lyonsite-type vanadates are known at the present time other than the namesake mineral. It is possible, indeed likely, that the high-pressure lyonsite variation of the structure exists for these stoichiometric compositions as well. Additionally, it is possible that the lyonsite structure was not formed because of the off-cation stoichiometric compositional range for the lyonsite-type vanadates. That is, there are potentially numerous lyonsite-type vanadates that simply have not been discovered owing to the off-stoichiometric cation ratios caused by the aforementioned cation vacancies. For example, while attempts to form α-$Cu_3Fe_4(VO_4)_6$ resulted in β-$Cu_3Fe_4(VO_4)_6$,[41] the off-stoichiometric phase, $Cu_4Fe_{3.333}(VO_4)_6$, adopts the lyonsite-type structure.[39] Both compositions lie on the $Cu_{3+1.5x}Fe_{4-x}(VO_4)_6$ phase line, suggesting some off-stoichiometric range of existence for the lyonsite-type compounds and a transition between the two structures somewhere along the tie line. It was found that the lyonsite-type phase exists for the compositional range $0.667 \le x \le 0.778$ for $Cu_{3+1.5x}Fe_{4-x}(VO_4)_6$. Similarly, $Co_3Fe_4(VO_4)_6$ has been described as having the β-$Cu_3Fe_4(VO_4)_6$ structure type by comparing powder diffraction patterns.[44] However, $Co_4Fe_{3.33}(VO_4)_6$ has the lyonsite structure type,[37] and again, both compositions lie on the $Co_{3+1.5x}Fe_{4-x}(VO_4)_6$ phase line. It is certainly possible that further investigations of other $A_{3+1.5x}B_{4-x}(VO_4)_6$ compositional ranges will yield similar results.

As suggested above, the $Fe_7(PO_4)_6$ structure type represents another large class of materials,[45] and could itself be the focus of new solid-state chemistry. For a short explanation of how various elemental compositions and structures are related within the $Fe_7(PO_4)_6$ structure type, the reader is referred to reference [41]. Perhaps one reason why the $Fe_7(PO_4)_6$ structure is preferred at ambient pressure is because cation vacancies are necessary to form lyonsite-type vanadates with a stoichiometric $A_3B_4(VO_4)_6$ formula, but are not necessary when the $Fe_7(PO_4)_6$ structural framework is used. The special role of cation vacancies will be discussed in the next section. Similar to the vanadates, it is likely that many phosphates and arsenates will form the lyonsite structure with some combination of pressure and off-stoichiometric cation ratios.

Tungstates and vanadotungstates: There are two tungsten lyonsite type analogues to date: $Li_2Mg_2(WO_4)_3$[46,47] and $Mg_{2.5}VWO_8$.[48] Interestingly, in reporting $Mg_{2.5}VWO_8$, the

authors reported unsuccessful attempts to substitute other divalent cations for Mg^{2+}. Other stoichiometries within the ternary Li_2O–MO_x–WO_3 phase system such as $LiM(WO_4)_2$ (M = Fe, Ga, Sc, In)[49] and $Li_2M(WO_4)_2$ (M = Co, Ni, Cu)[50] are known, but the $Li_2M_2(WO_4)_3$ stoichiometry is unknown for any element other than magnesium. More research is needed to understand the relative stability of the lyonsite crystalline framework for tungsten versus molybdenum.

Crystallographic Relationships, Structural Connectivity, and Cation Vacancies

It is rather amazing that seemingly unrelated materials such as α-$Cu_3Fe_4(VO_4)_6$ and $Li_2Mg_2(MoO_4)_3$, with completely different stoichiometries, elemental compositions, and cation charges are members of the same homeotypic family. The two phases α-$Cu_3Fe_4(VO_4)_6$ and $Li_2Mg_2(MoO_4)_3$ have been chosen to illustrate the crystallographic relationship between phases with such different compositions. This relationship is summarized in Table 3. The lyonsite structure is orthorhombic, space group *Pnma*, and the general formula can be written as $A_{16}B_{12}O_{48}$. There are three unique A sites (two octahedra and one trigonal prism), two unique B sites (two tetrahedra), and seven unique oxygen sites (see Table 3). The tetrahedral (B) positions are fully occupied by either V^{5+} or Mo^{6+} in α-$Cu_3Fe_4(VO_4)_6$ or $Li_2Mg_2(MoO_4)_3$, respectively, on positions with site multiplicities of four and eight, for a total of twelve tetrahedral positions in the unit cell.

Table 3. α-$Cu_3Fe_4(VO_4)_6$ and $Li_2Mg_2(MoO_4)_3$ comparison.

α-$Cu_3Fe_4(VO_4)_6$	Multiplicity	$Li_2Mg_2(MoO_4)_3$
Fe1	8d	Li/Mg1[b]
Cu1[a]	4c	Li/Mg2[c]
Cu2	4c	Li/Mg3[d]
V1	4c	Mo1
V2	8d	Mo2
O2	8d	O1
O6	4c	O2
O4	8d	O3
O3	4c	O4
O1	8d	O5
O5	8d	O6
O7	8d	O7

[a] Half occupied. [b] 0.659 Mg/0.341 Li. [c] 0.471 Mg/0.529 Li. [d] 0.210 Mg/0.790 Li.

Generally, the A site is composed of two different cations of different oxidation state; here Cu^{2+}/Fe^{3+} and Li^+/Mg^{2+}. The three AO_6 positions have site multiplicities of 8d, 4c, and 4c, for a total of 16 A sites in the unit cell, hence the general formula $A_{16}B_{12}O_{48}$. In α-$Cu_3Fe_4(VO_4)_6$, Cu^{2+} ions occupy both of the 4c positions, while Fe^{3+} occupies the 8d position. This fully occupied model cannot be charge balanced, and thus, cation vacancies are present in the mineral. Specifically, half of the Cu(1) sites are vacant. Therefore, the formula for α-$Cu_3Fe_4(VO_4)_6$ could be written as "□$Cu_3Fe_4(VO_4)_6$" or "□$_2Cu_6Fe_8V_{12}O_{48}$", in which □ represents the cation vacancy. Similarly, in $Li_2Mg_2(MoO_4)_3$, Li^+ and Mg^{2+} are distributed statistically amongst the three AO_6 positions. In this case, the charge can be balanced with an even distribution of lithium and magnesium amongst the sixteen different A sites, and therefore, no cation vacancies are necessary, thus the formula $Li_2Mg_2Mo_3O_{12}$ can be rewritten as $Li_8Mg_8Mo_{12}O_{48}$. When □$_2Cu_6Fe_8V_{12}O_{48}$ and $Li_8Mg_8Mo_{12}O_{48}$ are written with the same oxygen stoichiometry and cation vacancies are considered, it is possible to realize and fully understand the relationship between the two phases that upon first glance, appear quite different.

The lyonsite structure is remarkably adaptable, in part, because of the ability to incorporate varying amounts of cation vacancies. The percent of A site cation vacancies for various stoichiometries are listed in Table 2. To understand the typical positioning of the cation vacancies, a more detailed structural investigation is helpful. The structure is formed from isolated tetrahedra linked by octahedra and trigonal prisms that form zigzag sheets and columns, respectively (see Figure 1). These sheets and columns share corners and form hexagonal tunnels. The connectivity of the AO_6 polyhedra that form the hexagonal tunnels is depicted in Figure 2. The isolated tetrahedra are joined to the inner wall of the hexagonal tunnels, and infinite chains of face-shared octahedra (see Figure 3) pass through the center of the tunnels. The cation vacancies are localized on these infinite chains of face-shared octahedra, thereby minimizing the coulombic repulsions associated with the close partitioning of cations within the infinite chain. The face-shared cat-

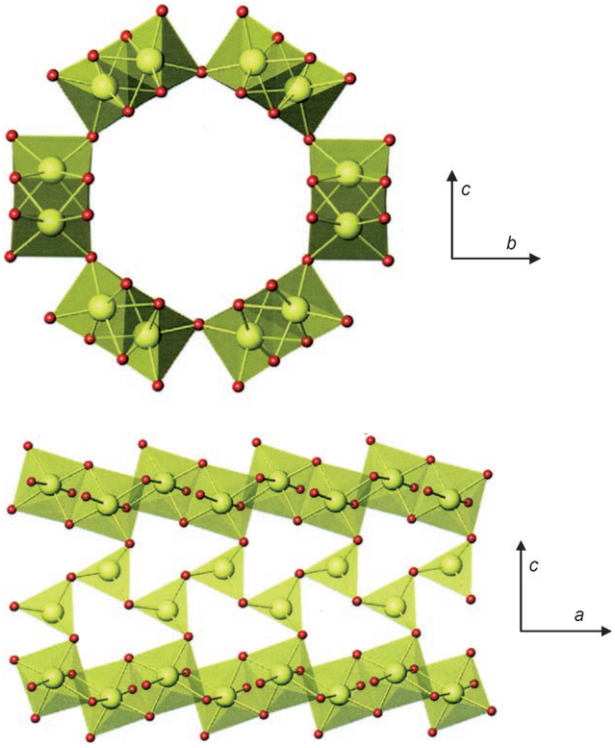

Figure 2. Top: The hexagonal tunnel formed by AO_6 polyhedra. Bottom: The connectivity of the AO_6 polyhedra that form the hexagonal tunnel.

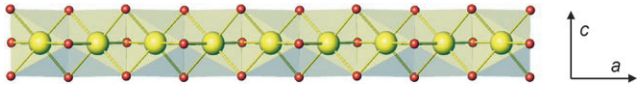

Figure 3. The infinite chain of face shared AO_6 octahedra.

ions are very close together (~2.5 Å), and the crystallographic *a* axis is twice the length of this M^{n+}–M^{n+} distance.

Variable compositions and solid solutions are possible because the crystalline framework can tolerate an appreciable level of cation vacancies. All of the lyonsite-type vanadates contain vacancies, giving variable stoichiometries such as $Co_{3+1.5x}Fe_{4-x}(VO_4)_6$ and $Cu_{3+1.5x}Fe_{4-x}(VO_4)_6$. Although the $Li_2M_2(MoO_4)_3$ and $Li_3M(MoO_4)_3$ compounds do not contain cation vacancies, it has been demonstrated that vacancies can be introduced with solid solutions such as $Li_{2-2x}Mg_{2+x}(MoO_4)_3$ $(0 \le x \le 0.3)$,[19] $Na_{2-2x}Co_{2+x}(MoO_4)_3$,[14] and $Na_{2-2x}Zn_{2+x}(MoO_4)_3$.[14]

In addition to vanadates and molybdates, variable compositions are also observed in the mixed vanadomolybdates and vanadotungstates. A considerable solid solution was found to exist in the subsolidus phase equilibria of the MgO-V_2O_5-MoO_3 system as $Mg_{2.5+x}V_{1+2x}Mo_{1-2x}O_8$ $(-0.05 \le x \le 0.05)$,[32] and the exact crystal compositions of $Mg_{2.5}VMoO_8$ $(Mg_{2.54}V_{1.08}Mo_{0.92}O_8)$,[32] $Mn_{2.5}VMoO_8$ $(Mn_{2.47}V_{0.94}Mo_{1.06}O_8)$,[34] $Zn_{2.5}VMoO_8$ $(Zn_{3.77}V_{1.54}Mo_{1.46}O_8)$,[35] and $Mg_{2.5}VWO_8$ $(Mg_{2.56}V_{1.12}W_{0.88}O_8)$ were found to be off-stoichiometric. It is likely then, that the concentration of cation vacancies can be systematically varied in each of these single-phase materials by using the general equation $M_{2.5+x}V_{1+2x}(Mo,W)_{1-2x}O_8$. These are, however, limited ranges of solubility. For example, $Mg_{2.5}VMoO_8$, with $Z=6$, can be written as $Mg_{15}V_6Mo_6O_{48}$. The twelve tetrahedral positions are fully occupied (6 V and 6 Mo), and 15 of the 16 Mg positions are occupied. Therefore, the formula can be written as $\square Mg_{15}V_6Mo_6O_{48}$ or $\square_{0.1667}Mg_{2.5}VMoO_8$. According to the formula $Mg_{2.5+x}V_{1+2x}Mo_{1-2x}O_8$, a fully occupied model would have the stoichiometry "$Mg_{2.667}V_{1.333}Mo_{0.667}O_8$". Interestingly, at the conditions reported for the synthesis, the solid solution was found to exist for the range $-0.05 \le x \le 0.05$, indicating that in some structures, the vacancies are well tolerated by the crystal framework.

In contrast to $Mg_{2.5}VMoO_8$, in which the vacancies cannot be completely removed, vacancies can be systematically removed in the solid solution $\square_{1/4-x/6}Li_{4x/3}Mg_{15/4-7x/6}V_{3/2-x}Mo_{3/2+x}O_{12}$ $(0 \le x \le 1.5)$, in which Mo^{6+} and V^{5+} can be substituted for each other with charge neutrality maintained by varying the vacancy/lithium/magnesium ratio.[51] Remarkably, a complete solid solution exists between the two end-member phases of the solid solution $Mg_{2.5}VMoO_8$ and $Li_2Mg_2(MoO_4)_3$, for which every stoichiometry along the tie line maintains a composition in which one lyonsite type phase is observed. This is one of the best examples illustrating the diversity and adaptive nature of this structure. Similar solid solutions almost certainly will be formed for other systems such as $M_{2.5}VMoO_8$–$Li_2M_2(MoO_4)_3$ (M = Mn, Co, Zn).

Removing an A cation perturbs not only the cation distribution, but also the oxygen framework. In fully occupied lyonsite type structures, each oxygen atom is three-coordinate, bonded twice to an AO_6-centered cation and once to a BO_4-centered cation. A vacancy on the face-shared octahedral position decreases the coordination of the oxygen atoms surrounding the vacancy to two, bonded once to an AO_6-centered cation and once to a BO_4-centered cation. The under coordinated oxygen atoms can satisfy bond valence by displacing toward the higher oxidation state transition-metal cation. For example, in $Mg_{2.5}VMoO_8$, in which the infinite chains of face-shared octahedra are occupied by Mg^{2+} ions, the crystallographic bond lengths of Mo–O bonds surrounding the vacancies are significantly shorter than the other tetrahedral bond lengths.[32] In fact, Raman spectroscopy revealed that higher order bond interactions are likely formed.

It would be valuable, then, to synthesize structures with higher oxidation state metal cations occupying the infinite chains of face-shared octahedra to provide a structural comparison. The higher oxidation state cation should provide a stronger binding interaction between itself and the under coordinated oxygen. In addition, high-oxidation-state cations in this position further promote the concept of lyonsite as an adaptable framework structure. The new lyonsite type oxides $Li_{2.82}Hf_{0.795}Mo_3O_{12}$ and $Li_{3.35}Ta_{0.53}Mo_3O_{12}$ have been prepared and their structures determined, demonstrating that the A site can accommodate metal cations over the range of oxidation states +1 to +5.

Li_2O–MO_x–MoO_3 (M = Hf, Ta, Nb) Phase Relations

As mentioned, the overall lyonsite-type molybdate formula can be written as $A_4Mo_3O_{12}$, in which A is a combination of +1, +2, and +3 metal ions. If an ion of oxidation state higher than +3 is used for the A site, then electrical neutrality must be maintained by either cation vacancies or off-stoichiometry. Therefore, a lyonsite-type single phase in the Li_2O–HfO_2–MoO_3 system should be possible, described by $\square_{1-3x}Li_{2+4x}Hf_{1-x}Mo_3O_{12}$. A mixture of Li_2MoO_4, HfO_2, and MoO_3 corresponding to a nominal stoichiometry of "$\square Li_2HfMo_3O_{12}$" ($x=0$, maximum vacancies) heated at 500 °C for 24 h produced the desired lyonsite-type phase with an excess of HfO_2. Conversely, a mixture of Li_2MoO_4, HfO_2, and MoO_3 corresponding to a stoichiometry of "$Li_{3.33}Hf_{0.67}Mo_3O_{12}$" ($x=1/3$, no vacancies) heated at 500 °C for 24 h resulted in the desired lyonsite type phase with an excess of Li_2MoO_4. The solid solution at 500 °C does not extend to the end members, but exists within a limited range. The range, as judged from powder X-ray diffraction, is $0.19 \le x \le 0.22$. Although it has been suggested that both the compositions "$Li_2Hf(MoO_4)_3$" and "$Li_{3.33}Hf_{0.67}Mo_3O_{12}$" ($Li_{10}Hf_2(MoO_4)_9$) are single phases from powder diffraction (see Table 2), this seems unlikely although results can depend on the synthesis conditions.

To date, no pentavalent cation has been observed on the A site in lyonsite structures. However, similar to the Li_2O–HfO_2–MoO_3 system, single-phase compositions potentially exist on the phase line described by the solid solution $\square_{2-4x}Li_{1+5x}Ta_{1-x}Mo_3O_{12}$. A nominal stoichiometry of "$Li_{3.5}Ta_{0.5}Mo_3O_{12}$" ($x=0.5$, no vacancies) was heated at 550 °C, producing a mixture of the desired lyonsite phase with Li_2MoO_4 in excess. A nominal stoichiometry of "$\square_2LiTaMo_3O_{12}$" ($x=0$, maximum vacancies) heated at 550 °C gave a mixture of $LiTaMoO_6$ and MoO_3. Again similar to the Li_2O-HfO_2-MoO_3 system, the solid solution does not extend to the end members. The solid solution range at 550 °C for the formula $\square_{2-4x}Li_{1+5x}Ta_{1-x}Mo_3O_{12}$ is $0.40 \leq x \leq 0.47$ as determined from powder X-ray diffraction.

Although crystals suitable for single-crystal X-ray diffraction have not been obtained as yet, it is clear from powder diffraction that a lyonsite-type phase exists in the Li_2O–Nb_2O_5–MoO_3 system. Similar to the Li_2O-Ta_2O_5-MoO_3 system, the solid solution range at 550 °C for the formula $\square_{2-4x}Li_{1+5x}Nb_{1-x}Mo_3O_{12}$ is $0.40 \leq x \leq 0.47$ as determined from powder X-ray diffraction.

Description of $Li_{2.82}Hf_{0.795}Mo_3O_{12}$ and $Li_{3.35}Ta_{0.53}Mo_3O_{12}$ Structures

The crystal structure of $Li_{2.82}Hf_{0.795}Mo_3O_{12}$ is identical to other lyonsite-type compounds and consists of two crystallographically non-equivalent mixed Li/Hf octahedral sites and one LiO_6 trigonal prismatic position surrounded by two crystallographically non-equivalent isolated MoO_4 tetrahedra (see Figure 4). Chains of both edge-sharing LiO_6 trigonal prisms and edge-sharing MO_6 octahedra are linked by isolated MoO_4 tetrahedra and form pseudohexagonal tunnels along the *a* axis (see Figure 2). Infinite columns of face sharing $M(2)O_6$ octahedra pass through the center of the tunnels (see Figure 3), with 38.5% of the positions vacant owing to the coulombic repulsions associated with the close partitioning of face-shared cations.

All oxygen atoms are three-coordinate (discounting cation vacancies), and each are bound to one molybdenum and two hafnium and/or lithium atoms. $M(1)O_6$ is joined to $Li(3)O_6$ by sharing corners. Both $Mo(1)O_4$ and $Mo(2)O_4$ tetrahedra are connected to the $M(1)O_6$ octahedra by sharing corners, while LiO_6 prisms share corners with only the $Mo(2)O_4$ tetrahedra.

The structure of $Li_{3.35}Ta_{0.53}Mo_3O_{12}$ is shown in Figure 5. The connectivity is identical to that of $Li_{2.82}Hf_{0.795}Mo_3O_{12}$

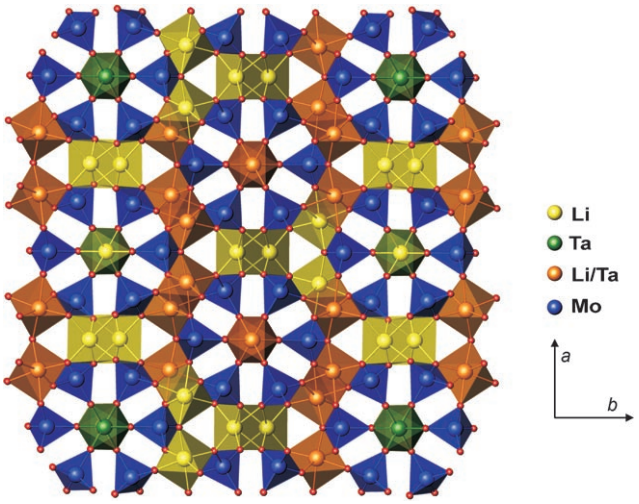

Figure 5. Structure of $Li_{3.35}Ta_{0.53}(MoO_4)_3$.

and other lyonsite-type materials. However, a loss of symmetry that reduces the space group from *Pnma* to $Pmn2_1$ can be attributed to the placement of Ta(1) and Li(9) on distinct positions in the infinite chains of face-shared octahedra down the center of the hexagonal tunnels. This cation order, coupled with the cation vacancies on the Li(9) position, probably occurs to minimize the coulombic repulsions that would be associated with placing pentavalent cations in such close proximity (2.5 Å). Additionally, the Ta(1)/Li(9) order reduces a mirror plane seen in $Li_{2.82}Hf_{0.795}Mo_3O_{12}$ to a 2_1 screw axis in $Li_{3.35}Ta_{0.53}Mo_3O_{12}$ (see Figure 6), and doubles the *b* axis of $Li_{2.82}Hf_{0.795}Mo_3O_{12}$ (10.6517 Å) in

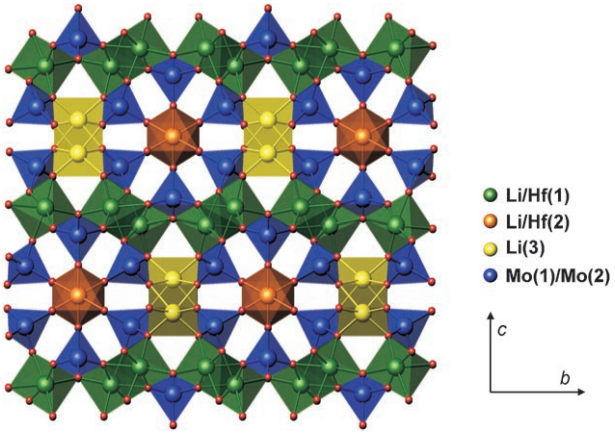

Figure 4. Structure of $Li_{2.82}Hf_{0.795}(MoO_4)_3$.

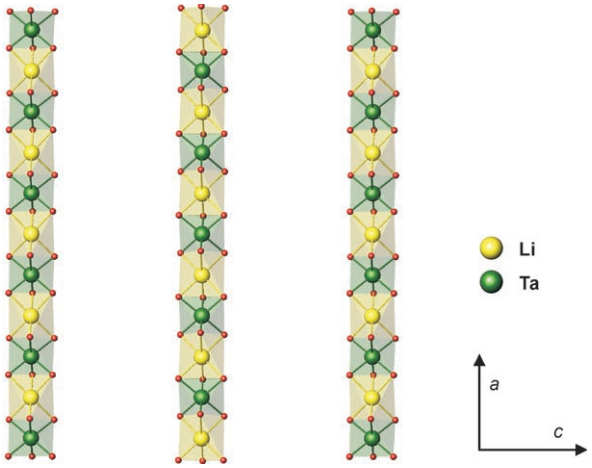

Figure 6. The infinite chains of face-shared octahedra in $Li_{3.35}Ta_{0.53}(MoO_4)_3$.

$Li_{3.35}Ta_{0.53}Mo_3O_{12}$ (21.1089 Å, becoming the *a* axis in $Li_{3.35}Ta_{0.53}Mo_3O_{12}$ after the space group is set in standard form). The *a* and *c* axes remain unchanged. This is further illustrated in Figure 6.

A similar symmetry reduction ($Pnma \rightarrow Pmn2_1$) pattern and doubling of one lattice constant have been observed previously for $Li_2Zr(MoO_4)_3$. One might expect similarly charged Hf^{4+} to behave like Zr^{4+} and adopt the $Pmn2_1$ space group. However, $Li_{2.82}Hf_{0.795}Mo_3O_{12}$ retains the higher symmetry space group. Because $Li_{2.82}Hf_{0.795}Mo_3O_{12}$ is in the higher symmetry space group, there is no crystallographic ordering of the face-shared cations and vacancies. However, the site occupancy suggests that Hf^{4+} is most likely alternating predominately with vacancies. It appears that the higher oxidation state cations show a tendency to systematically order themselves down the hexagonal tunnels on the face-shared positions. The order places either Li^+ or cation vacancies on both sides of the high-oxidation-state cations, which serves to reduce the repulsions that would be associated with close partitioning of face-shared cations of such high oxidation states.

As expected, in both $Li_{2.82}Hf_{0.795}Mo_3O_{12}$ and $Li_{3.35}Ta_{0.53}Mo_3O_{12}$, the longest crystallographic Mo–O bond lengths always correspond to the Mo–O bonds that surround the cation vacancies. This is in contrast to the short average bond lengths that were described previously for the Mo–O bonds surrounding the cation vacancies in $Mg_{2.5}VMoO_8$. The bond lengths for $Li_{2.82}Hf_{0.795}Mo_3O_{12}$ and $Li_{3.35}Ta_{0.53}Mo_3O_{12}$ are listed in Tables 4 and 5, respectively. This may be expected because all of the vacant positions are missing Li^+ ions. Both the Hf^{4+} and Ta^{5+} site occupancy along the infinite chains of face-shared octahedra is ~50%. This corresponds to Hf^{4+} and Ta^{5+} ions bordered by either □ or Li^+, as previously discussed. Therefore, a Li^+ vacancy would leave a very high oxidation state metal cation sharing the under coordinated oxygen with Mo^{6+}. The under coordinated oxygen atom does not need to displace toward the Mo^{6+} in order to maintain its bond valence, as is necessary when Mg^{2+} shares the under coordinated oxygen with Mo^{6+}.

Table 4. Selected bond lengths for $Li_{2.82}Hf_{0.795}Mo_3O_{12}$.

Mo(1)–O(5)	1.774(2)	Hf/Li(1)–O(3)	2.0732(18)
Mo(1)–O(6)×2	1.7582(17)	Hf/Li(1)–O(3)	2.1451(18)
Mo(1)–O(7)	1.795(2)	Hf/Li(1)–O(4)	2.0942(17)
		Hf/Li(1)–O(5)	2.1274(13)
Mo(2)–O(1)	1.7358(17)	Hf/Li(1)–O(6)	2.1005(17)
Mo(2)–O(2)	1.8047(17)	Hf/Li(1)–O(6)	2.2526(18)
Mo(2)–O(3)	1.7731(18)		
Mo(2)–O(4)	1.7616(17)	Hf/Li(2)–O(2)×2	2.0908(17)
		Hf/Li(2)–O(2)×2	2.1103(17)
		Hf/Li(2)–O(7)	2.137(2)
		Hf/Li(2)–O(7)	2.145(2)
		Li(3)–O(1)×2	2.174(5)
		Li(3)–O(1)×2	2.261(5)
		Li(3)–O(4)×2	2.133(5)

The experimental details of synthesis and X-ray crystallographic characterization of $Li_{2.82}Hf_{0.795}Mo_3O_{12}$ and $Li_{3.35}Ta_{0.53}Mo_3O_{12}$ are given in the Supporting Information. Further details of the crystal structure investigations can be obtained from the Fachinformationszentrum Karlsruhe, 76344 Eggenstein-Leopoldshafen, Germany (fax: (+49) 7247-808-666; e-mail: crysdata@fiz-karlsruhe.de) on quoting the depository numbers CSD-416278 ($Li_{2.82}Hf_{0.795}Mo_3O_{12}$) and CSD-416279 ($Li_{3.35}Ta_{0.53}(MoO_4)_3$).

Structural Variations

Variations in structure within a particular structural family are not unusual. For example, $SrTiO_3$ is cubic while $CaTiO_3$

Table 5. Selected bond lengths for $Li_{3.35}Ta_{0.53}Mo_3O_{12}$.

Mo(1)–O(4)	1.867(11)	Mo(2)–O(3)	1.876(8)	Mo(3)–O(1)	1.763(9)	Mo(4)–O(2)	1.861(11)
Mo(1)–O(6)	1.743(9)×2	Mo(2)–O(7)	1.717(11)	Mo(3)–O(9)	1.746(9)	Mo(4)–O(5)	1.743(14)
Mo(1)–O(13)	1.730(13)	Mo(2)–O(10)	1.755(8)	Mo(3)–O(11)	1.723(10)	Mo(4)–O(8)	1.756(9)×2
		Mo(2)–O(12)	1.762(8)	Mo(3)–O(14)	1.846(8)		
Mo(5)–O(15)	1.873(8)	Mo(6)–O(19)	1.867(8)	Mo(7)–O(23)	1.772(12)	Ta(1)–O(2)	1.992(13)
Mo(5)–O(16)	1.771(10)	Mo(6)–O(20)	1.779(10)	Mo(7)–O(24)	1.729(9)	Ta(1)–O(3)	1.957(8)×2
Mo(5)–O(17)	1.727(10)	Mo(6)–O(21)	1.715(10)	Mo(7)–O(25)	1.740(9)	Ta(1)–O(4)	1.936(12)
Mo(5)–O(18)	1.723(10)	Mo(6)–O(22)	1.731(10)	Mo(7)–O(26)	1.867(8)	Ta(1)–O(14)	1.953(9)×2
Li(2)–O(1)	2.139(11)	Li(3)–O(1)	2.101(19)	Li(4)–O(6)	2.240(11)	Li(5)–O(15)	2.042(10)
Li(2)–O(5)	2.091(11)	Li(3)–O(8)	2.216(15)	Li(4)–O(7)	2.064(12)	Li(5)–O(15)	1.996(10)
Li(2)–O(8)	2.094(13)	Li(3)–O(11)	2.122(16)	Li(4)–O(12)	2.053(15)	Li(5)–O(19)	1.990(10)
Li(2)–O(20)	2.083(12)	Li(3)–O(21)	2.130(16)	Li(4)–O(18)	2.121(13)	Li(5)–O(19)	2.038(10)
Li(2)–O(21)	2.072(15)	Li(3)–O(23)	2.116(16)	Li(4)–O(23)	2.149(12)	Li(5)–O(26)	2.027(11)
Li(2)–O(25)	2.232(12)	Li(3)–O(25)	2.07(2)	Li(4)–O(24)	2.109(15)	Li(5)–O(26)	2.059(11)
Li(6)–O(16)	2.07(2)×2	Li(7)–O(6)	2.09(3)	Li(8)–O(7)	2.17(3)	Li(9)–O(2)	2.057(13)
Li(6)–O(17)	2.22(3)×2	Li(7)–O(12)	2.07(2)	Li(8)–O(9)	2.34(3)	Li(9)–O(3)	2.113(9)×2
Li(6)–O(22)	2.25(3)×2	Li(7)–O(13)	2.18(2)	Li(8)–O(9)	2.15(4)	Li(9)–O(4)	2.219(13)
		Li(7)–O(16)	2.11(2)	Li(8)–O(10)	2.07(4)	Li(9)–O(14)	2.081(9)×2
		Li(7)–O(18)	2.13(3)	Li(8)–O(10)	2.18(3)		
		Li(7)–O(24)	2.22(2)	Li(8)–O(11)	2.23(3)		

is orthorhombic, but both exhibit the same connectivity identical with the perovskite structure. Similar structural distortions and variations occur within the lyonsite crystalline lattice. Although the majority of lyonsite-type oxides are in the orthorhombic space group *Pnma*, several structures with the lyonsite-type connectivity are known with lower symmetry. The orthorhombic crystal class is generally preserved, and subclasses of the *Pnma* space group are observed. For example, $Li_2Zr(MoO_4)_3$ and $Li_{3.35}Ta_{0.53}(MoO_4)_3$ crystallize in the space group $P2_1mn$ ($Pmn2_1$), while $Cu_{3.85}Mo_3O_{12}$ and $Zn_{3.77}V_{1.54}Mo_{1.46}O_8$ crystallize in the space group $P2_12_12_1$.

The origin of the symmetry reduction is understood for $Li_2Zr(MoO_4)_3$ and $Li_{3.35}Ta_{0.53}(MoO_4)_3$. In $Li_2Zr(MoO_4)_3$, the face-shared octahedral position is ordered with Zr^{4+} ions alternating with cation vacancies, which results in the doubling of one of the lattice constants and the loss of a mirror plane. Likewise, Ta^{5+} ions alternate with Li^+ ions in $Li_{3.35}Ta_{0.53}(MoO_4)_3$. In contrast, it is unclear why the distortion to the $P2_12_12_1$ space group occurs. It has been suggested that a distortion of the trigonal prismatic environment causes the loss of symmetry, although the origin of this distortion is unknown.[35]

Properties

Adaptable framework structures can have different properties because of the varying elemental compositions. To date, the lyonsite structure type has been investigated for two properties: ionic conduction and catalysis. High electrical conductivity was first observed for $Li_2Cu_2(MoO_4)_3$ in 1981,[52] and a significant effort has since been made to investigate the conductivity of many of the molybdates.[19,53–58] The lyonsite structure fits the criteria for NASICON ion conductors owing to the arrangement of the isolated $(MO_4)^{n-}$ polyanion tetrahedra. A review of various families of $A_xB_y(MoO_4)_z$ molybdate families discusses the ionic conduction of lyonsite type molybdates.[10]

The surface of various mixed metal oxide vanadates and molybdates with $(VO_4)^{3-}$ and $(MoO_4)^{2-}$ tetrahedral units has been shown to be active for hydrocarbon oxidations.[59–63] Containing both $(VO_4)^{3-}$ and $(MoO_4)^{2-}$ polyhedral units, the mixed vanadomolybdate lyonsite-type phase $Mg_{2.5}VMoO_8$ was demonstrated to be active for the oxidative dehydrogenation of butane and propane.[33,63] These catalytic properties are cited as motivation for the exploratory synthesis of lyonsite-type compounds, but only $Mg_{2.5}VMoO_8$ has been tested. Recently $Mg_{2.5}VMoO_8$ and $Zn_{2.5}VMoO_8$ have been studied as photocatalysts.[64]

Conclusion

The lyonsite crystal framework constitutes a large family of materials, spanning a wide range of elements, oxidation states, and cation stoichiometries similar to other important structure types such as perovskite, garnet, apatite, and spinel. The use of cation vacancies and off-cation stoichiometry by lyonsite-type oxides contributes to this remarkably adaptive structure type. The crystal structures of the lyonsite type molybdates $Li_{2.82}Hf_{0.795}Mo_3O_{12}$ and $Li_{3.35}Ta_{0.53}Mo_3O_{12}$ have been determined, and are consistent with other known lyonsite-type phases.

Acknowledgements

The authors gratefully acknowledge the National Science Foundation, Solid State Chemistry (Award Nos. DMR-9727516 and DMR-0312136), the EMSI program of the National Science Foundation at the Northwestern University Institute for Environmental Catalysis (Grant No. 9810378), and the Department of Energy, BES-Chemical Sciences, Geosciences, and Biosciences Division under grant No. DE-FG0203ER15457 for support of this work, and made use of the Central Facilities supported by the MRSEC program of the National Science Foundation (Grant DMR-0076097) at the Materials Research Center of Northwestern University.

[1] M. T. Anderson, J. T. Vaughey, K. R. Poeppelmeier, *Chem. Mater.* **1993**, *5*, 151–165.
[2] M. T. Anderson, K. B. Greenwood, G. A. Taylor, K. R. Poeppelmeier, *Prog. Solid State Chem.* **1993**, *22*, 197–233.
[3] S. Geller, *Z. Kristallogr. Kristallgeom. Kristallphys. Kristallchem.* **1967**, *125*, 1–47.
[4] N. W. Grimes, *Spectrum* **1976**, *14*, 27–30.
[5] C. P. Khattak, F. F. Y. Wang, *Handb. Phys. Chem. Rare Earths* **1979**, *3*, 525–607.
[6] E. Pollert, *React. Solids* **1988**, *5*, 279–291.
[7] C. N. R. Rao, *Physica C* **1988**, *153–155*, 1762–1768.
[8] T. J. White, D. ZhiLi, *Acta Crystallogr. Sect. B* **2003**, *59*, 1–16.
[9] J. M. Hughes, S. J. Starkey, M. L. Malinconico, L. L. Malinconico, *Am. Mineral.* **1987**, *72*, 1000–1005.
[10] S. S. Solodovnikov, R. F. Klevtsova and P. V. Klevtsov, *Zh. Strukt. Khim.* **1994**, *35*, 145–157.
[11] R. D. Shannon, C. T. Prewitt, *Acta Crystallogr. Sect. B* **1969**, *25*, 925–946.
[12] J. A. Ibers, G. W. Smith, *Acta Crystallogr.* **1964**, *17*, 190–197.
[13] R. F. Klevtsova, S. A. Magarill, *Kristallografiya* **1970**, *15*, 710–715.
[14] V. A. Efremov, V. K. Trunov, *Zh. Neorg. Khim.* **1972**, *17*, 2034–2039.
[15] V. G. Penkova, P. V. Klevtsov, *Zh. Neorg. Khim.* **1977**, *22*, 1713–1715.
[16] V. K. Trunov, *Zh. Neorg. Khim.* **1971**, *16*, 553–554.
[17] B. M. Wanklyn, F. R. Wondre, W. Davison, *J. Mater. Sci.* **1976**, *11*, 1607–1614.
[18] S. F. Solodovnikov, Z. A. Solodovnikova, R. F. Klevtsova, L. A. Glinskaya, P. V. Klevtsov, E. S. Zotova, *Zh. Strukt. Khim.* **1994**, *35*, 136–144.
[19] L. Sebastian, Y. Piffard, A. K. Shukla, F. Taulelle, J. Gopalakrishnan, *J. Mater. Chem.* **2003**, *13*, 1797–1802.
[20] M. Wiesmann, I. Svoboda, H. Weitzel, H. Fuess, *Z. Kristallogr.* **1995**, *210*, 525.
[21] M. Ozima, S. Sato, T. Zoltai, *Acta Crystallogr. Sect. B* **1977**, *33*, 2175–2181.
[22] M. Ozima, T. Zoltai, *J. Cryst. Growth* **1976**, *34*, 301–303.
[23] P. V. Klevtsov, *Kristallografiya* **1970**, *15*, 797–802.
[24] V. K. Trunov, V. A. Efremov, *Zh. Neorg. Khim.* **1971**, *16*, 2026–2027.
[25] M. A. Juri, M. Viola, G. Narda, J. C. Pedregosa, *Acta Cient. Venez.* **1992**, *43*, 14–18.
[26] U. Kolitsch, E. Tillmanns, *Acta Crystallogr. Sect. E* **2003**, *59*, i55–i58.
[27] P. V. Klevtsov, E. S. Zolotova, *Izv. Akad. Nauk SSSR Neorg. Mater.* **1973**, *9*, 79–82.
[28] R. F. Klevtsova, A. A. Antonova, L. A. Glinskaya, *Kristallografiya* **1979**, *24*, 1043–1047.

[29] M. A. Juri, M. Viola, J. C. Pedregosa, *Acta Sud Am. Quim.* **1984**, *4*, 37–45.
[30] L. Katz, A. Kasenally, L. Kihlborg, *Acta Crystallogr. Sect. B* **1971**, *27*, 2071–2077.
[31] V. G. Zubkov, I. A. Leonidov, K. R. Poeppelmeier, V. L. Kozhevnikov, *J. Solid State Chem.* **1994**, *111*, 197–201.
[32] X. Wang, C. L. Stern, K. R. Poeppelmeier, *J. Alloys Compd.* **1996**, *243*, 51–58.
[33] W. D. Harding, H. H. Kung, V. L. Kozhevnikov, K. R. Poeppelmeier, *J. Catal.* **1993**, *144*, 597–610.
[34] X. Wang, K. R. Heier, C. L. Stern, K. R. Poeppelmeier, *J. Alloys Compd.* **1998**, *267*, 79–85.
[35] X. Wang, K. R. Heier, C. L. Stern, K. R. Poeppelmeier, *J. Alloys Compd.* **1997**, *255*, 190–194.
[36] M. Kurzawa, M. Bosacka, P. Jakubus, *J. Mater. Sci.* **2003**, *38*, 3137–3142.
[37] X. Wang, D. A. Vander Griend, C. L. Stern, K. R. Poeppelmeier, *Inorg. Chem.* **2000**, *39*, 136–140.
[38] A. A. Belik, F. Izumi, T. Ikeda, A. Nisawa, T. Kamiyama, K. Oikawa, *Solid State Sci.* **2002**, *4*, 515–522.
[39] A. A. Belik, A. P. Malakho, K. V. Pokholok, B. I. Lazoryak, *J. Solid State Chem.* **2001**, *156*, 339–348.
[40] A. P. Malakho, A. A. Belik, B. I. Lazoryak, *Zh. Neorg. Khim.* **2003**, *48*, 709–714.
[41] M. A. Lafontaine, J. M. Greneche, Y. Laligant, G. Ferey, *J. Solid State Chem.* **1994**, *108*, 1–10.
[42] Y. A. Gorbunov, B. A. Maksimov, Y. K. Kabalov, A. N. Ivashchenko, O. K. Mel'nikov, N. V. Belov, *Dokl. Akad. Nauk SSSR* **1980**, *254*, 873–877.
[43] M. Kurzawa, A. Blonska-Tabero, *Mater. Res. Bull.* **2002**, *37*, 849–858.
[44] M. Kurzawa, A. Blonska-Tabero, *J. Therm. Anal. Calorim.* **2004**, *77*, 17–24.
[45] A. A. Belik, K. V. Pokholok, A. P. Malakho, S. S. Khasanov, B. I. Lazoryak, *Zh. Neorg. Khim.* **2000**, *45*, 1633–1648.
[46] Z. Fu, W. Li, *Powder Diffr.* **1994**, *9*, 158–160.
[47] Z. Fu, W. Li, Y. Liu, J. Li, *Wuli Huaxue Xuebao* **1988**, *4*, 320–324.
[48] J. D. Pless, H.-S. Kim, J. P. Smit, X. Wang, P. C. Stair, K. R. Poeppelmeier, *Inorg. Chem.* **2006**, *45*, 514–520.
[49] P. V. Klevtsov, A. V. Demenev, R. F. Klevtsova, *Kristallografiya* **1971**, *16*, 520–526.
[50] M. Alvarez-Vega, J. Rodriguez-Carvajal, J. G. Reyes-Cardenas, A. F. Fuentes, U. Amador, *Chem. Mater.* **2001**, *13*, 3871–3875.
[51] J. P. Smit, H.-S. Kim, J. D. Pless, P. C. Stair, K. R. Poeppelmeier, *Inorg. Chem.* **2006**, *45*, 521–528.
[52] A. I. Korosteleva, V. I. Kovalenko, E. A. Ukshe, *Izv. Akad. Nauk SSSR, Neorg. Mater.* **1981**, *17*, 748–749.
[53] M. Alvarez-Vega, U. Amador, M. E. Arroyo-de Dompablo, *J. Electrochem. Soc.* **2005**, *152*, A1306–A1311.
[54] A. K. Ivanov-Shits, A. V. Nistyuk, N. G. Chaban, *Inorg. Mater.* **1999**, *35*, 756–758.
[55] K. M. Begam, M. S. Michael, Y. H. Taufiq-Yap, S. R. S. Prabaharan, *Electrochem. Solid-State Lett.* **2004**, *7*, A242–A246.
[56] K. M. Begam, S. Selladurai, M. S. Michael, S. R. S. Prabaharan, *Ionics* **2004**, *10*, 77–83.
[57] S. R. S. Prabaharan, A. Fauzi, M. S. Michael, K. M. Begam, *Solid State Ionics* **2004**, *171*, 157–165.
[58] S. R. S. Prabaharan, M. S. Michael, K. M. Begam, *Electrochem. Solid-State Lett.* **2004**, *7*, A416–A420.
[59] M. A. Chaar, D. Patel, M. C. Kung, H. H. Kung, *J. Catal.* **1987**, *105*, 483–498.
[60] M. A. Chaar, D. Patel, H. H. Kung, *J. Catal.* **1988**, *109*, 463–467.
[61] Y. S. Yoon, W. Ueda, Y. Moro-oka, *Top. Catal.* **1996**, *3*, 265–275.
[62] W. Ueda, Y.-S. Yoon, K.-H. Lee, Y. Moro-Oka, *Korean J. Chem. Eng.* **1997**, *14*, 474–478.
[63] J. D. Pless, B. B. Bardin, H.-S. Kim, D. Ko, M. T. Smith, R. R. Hammond, P. C. Stair, K. R. Poeppelmeier, *J. Catal.* **2004**, *223*, 419–431.
[64] D. Wang, Z. Zou, J. Ye, *Catal. Today* **2004**, *93–95*, 891–894.

Published online: June 6, 2006

